Biochemical and Biophysical Research Communications 426 (2012) 565–570

Contents lists available at SciVerse ScienceDirect

Biochemical and Biophysical Research Communications

journal homepage: www.elsevier.com/locate/ybbrc

Measuring intermolecular rupture forces with a combined TIRF-optical trap microscope and DNA curtains

Ja Yil Lee [a,b], Feng Wang [a,b], Teresa Fazio [d,1], Shalom Wind [d], Eric C. Greene [a,b,c,*]

[a] Department of Biochemistry and Molecular Biophysics, Columbia University, 650 West 168th Street, New York, NY 10032, USA
[b] Department of Biological Sciences, Columbia University, 650 West 168th Street, New York, NY 10032, USA
[c] Howard Hughes Medical Institute, Columbia University, 650 West 168th Street, New York, NY 10032, USA
[d] Department of Applied Physics and Applied Mathematics, Center for Electron Transport in Molecular Nanostructures, NanoMedicine Center for Mechanical Biology, Columbia University 1020 Schapiro CEPSR, 530 West 120th St., New York, NY 10027, USA

ARTICLE INFO

Article history:
Received 23 August 2012
Available online 4 September 2012

Keywords:
DNA curtains
Optical trap
Single-molecule
Combination
DNA pulling
Rupture force

ABSTRACT

We report a new approach to probing DNA–protein interactions by combining optical tweezers with a high-throughput DNA curtains technique. Here we determine the forces required to remove the individual lipid-anchored DNA molecules from the bilayer. We demonstrate that DNA anchored to the bilayer through a single biotin–streptavidin linkage withstands ~20 pN before being pulled free from the bilayer, whereas molecules anchored to the bilayer through multiple attachment points can withstand ⩾65 pN; access to this higher force regime is sufficient to probe the responses of protein–DNA interactions to force changes. As a proof-of-principle, we concurrently visualized DNA-bound fluorescently-tagged RNA polymerase while simultaneously stretching the DNA molecules. This work presents a step towards a powerful experimental platform that will enable concurrent visualization of DNA curtains while applying defined forces through optical tweezers.

1. Introduction

Single molecule measurements have proven to be powerful tools that provide unique insights into the underlying mechanisms of biological phenomena, many of which cannot be revealed through traditional ensemble biochemical or biophysical approaches [1,2]. Most single molecule techniques fit into two classes: those based upon the detection of a fluorescence signal [3,4], and those that rely upon force-based measurements [5–7]. There is a growing interest in combining these two types of different measurements [8–12].

To facilitate single molecule measurements, we have developed "DNA curtains" which utilize lipid bilayers, nano-fabricated barriers, and hydrodynamic flow to organize lipid-tethered DNA molecules into patterns on the surface of a microfluidic chamber [13–15]. These molecules can be visualized by total internal reflection fluorescence microscopy (TIRFM), allowing simultaneous observation of hundreds of individual molecules within a single field-of-view, and this experimental platform can be adapted to a number of biochemical problems related to protein–nucleic acid interactions [16–19].

Here we developed a TIRFM with an integrated optical trap, and using this combined TIRF-trap microscope we measured the rupture force of single lipids within a supported bilayer by pulling individual DNA molecules from DNA curtains. Optical tweezers have proven to be powerful tools applying precise forces (0.1–100 pN) on individual molecules and have been used to interrogate various biological processes [20–24]. We show that DNA molecules anchored to single lipids are pulled free from the bilayer with the application of ~20 pN. Increasing the number of attachment points on the bilayer allows the application of forces in excess of ~65 pN, expanding the applicability of DNA curtains to combined fluorescence and forced-based measurements with a force regime relevant to most protein–DNA interactions.

2. Materials and methods

2.1. DNA substrates

For single biotin or digoxigenin (dig) tags, λ-DNA (48,502-base pairs (bp); Invitrogen) was labeled at either end with oligonucleotides, as described [16]. For multiple tags, multiple biotin or dig tags were incorporated into a 1.4-kilobase λ-DNA fragment by PCR using low-fidelity Taq polymerase (Stratagene or Takara) along with biotin-dUTP (Roche) or dig-dUTP (Roche), respectively.

* Corresponding author at: Howard Hughes Medical Institute, Columbia University, 650 West 168th Street, New York, NY 10032, USA. Fax: +1 212 305 7932.
E-mail address: ecg2108@columbia.edu (E.C. Greene).
[1] Present address: Columbia Technology Ventures, 630 West 168th Street, New York, NY 10032, USA.

0006-291X/$ - see front matter © 2012 Elsevier Inc. All rights reserved.
http://dx.doi.org/10.1016/j.bbrc.2012.08.127

The PCR products were then ligated to connector oligonucleotides, bearing a sequence complementary to the 4-nt overhang by the ApaI along with a 12-nt sequence complementary to λ-DNA COS site. Excess connectors were removed with an S-400 HR column (GE Healthcare). The PCR products bearing the multiple biotin or dig tags (140 nM each) were ligated to the λ-DNA (4.2 nM) using T4 DNA ligase (4000U) and incubated overnight at room temperature. Finally, the λ-DNA was purified by passage through an S-1000 gel filtration column (GE Healthcare).

2.2. Fluorescent beads conjugated to antidigoxigenin antibodies

Fluorescent anti-dig-coated beads were prepared using *N*-(3-dimethylaminopropyl)-*N*′-ethylcarbodiimide hydrochloride (EDAC), *N*-hydroxysulfosuccinimide sodium salt (Sulfo-NHS) and carboxylated non-fluorescent polystyrene beads (diameter 1.5 μm; Bangslabs). Briefly, 10 pM of beads were prepared for labeling with successive washes of 10 mM NaOH, followed by H_2O. The carboxyl groups were then activated using 40 mg ml^{-1} EDAC (Sigma) and 25 mg ml^{-1} Sulfo-NHS (Sigma) in 0.1 M MES buffer (pH 5.5). The activated beads were then washed with 1× PBS (pH 7.4), and anti-dig (Novus Biological) and Alexa488-BSA (Invitrogen) were added to the beads at $\sim 3 \times 10^6$:1 and $\sim 3 \times 10^5$:1 M ratio, respectively. The reactions were then incubated with gentle agitation overnight at 4 °C. Finally, the beads were washed with buffer containing 1× PBS (pH 7.5), 1 mg ml^{-1} BSA, 10% glycerol, 0.1% azide, 0.1% Tween20, 1 mM EDTA, and 1 mM DTT and stored at 4 °C up to three months.

2.3. Microscope

Prism-type TIRFM was used for the fluorescence imaging (Fig. 1). Optical tweezers were combined with the TIRFM through the same objective lens, and an infrared-laser (1 W, 1064 nm; Crystalaser) was used for the optical trapping (Fig. 1B). The trap position was controlled by maneuvering a mirror mounted on motorized optical mount (8807; New Focus) and controlled remotely with iPicomotor modules (New Focus), and a telescopic lens system was adopted to maintain parallel beams such that the *z*-position of the trap did not move when the trap was moved in the *x* or *y*-directions. The IR beam entered the microscope through the back-port, and reflected toward the objective lens by a custom-made dichroic mirror (z780dcspxr; Chroma Technology), which transmits visible spectrum (400–800 nm) (Fig. 1C).

2.4. DNA pulling and rupture force

The bead trapping and DNA pulling were performed while observing the YOYO1-stained DNA and Alexa488-labeled bead by TIRFM. Individual bead-labeled DNA molecules were visually identified in the presence of buffer flow. The fluorescent bead attached to the end of a DNA was then captured with the IR laser trap, and buffer flow was then terminated. The DNA molecules were stretched at a constant rate of 5.3 μm s^{-1} until the molecules ruptured, as determined by visualization. The location of the biotinylated end of the DNA was obtained from the intersection the barrier and the DNA. The bead center position was obtained by fitting bead fluorescence with 2D Gaussian function, and the DNA extension was calculated by subtracting the bead radius from the distance between biotinylated DNA end and the center of the fluorescent bead DNA. The projection effect of the DNA extension was ignored because the length of DNA is much larger than the bead size.

The optical trap was controlled by maneuvering a remotely operated mirror. With this configuration, force measurements based on the trap stiffness and bead displacement cannot be obtained because the trap stiffness varies with the beam position. Moreover, the prism-type TIRFM geometry precludes use of back-focal-plane interferometry. Therefore, as an alternative to these approaches, the force exerted on the DNA was estimated using the well-established force vs extension curve of dsDNA [7,24,25]. The force vs extension curve is dependent on the salt concentration and the presence of intercalation dyes [26,27]. But under our salt condition (50–150 mM NaCl), the force vs extension curve is not sensitive to the ionic strength change [26] and we adopted the force vs extension curve measured at 150 mM Na^+ [24]. YOYO1, an intercalation dye, affects both mechanical and structural properties of dsDNA and hence changes the force vs extension curve [10,12,28]. A significant effect of YOYO1 on the force vs extension curve was previously reported at high YOYO1 concentration (>10 nM). However, Murade et al. reported that the force vs extension curve at 1 nM YOYO1 is not distinguished from that in the absence of YOYO1 [10]. Our experiments required only a low concentration of YOYO1 (0.1–0.2 nM), therefore, force vs extension curve of dsDNA should be reliable for the force estimation.

3. Results and discussion

3.1. DNA molecules labeled with single tags detached from the bilayer at low force

To make force measurements within DNA curtains we constructed a TIRF microscope with an integrated infrared optical trap (Fig. 1A and B). An optical trap could be used to stretch a single DNA by attaching a fluorescent bead to one end of DNA (Fig. 1A). Initial experiments utilized substrates labeled with single biotin and digoxigenin tags (Fig. 2). When the DNA molecules were stretched under hydrodynamic flow, those molecules harboring an anti-dig bead were readily distinguished by the bright signal from the bead (Fig. 2A, upper panel). At 0.1 ml min^{-1} flow rate, the DNA molecules lacking a fluorescent bead were stretched to ~12.5 μm in length ($\langle X \rangle / L = 0.78$), corresponding to ~0.5 pN of flow-induced force, whereas DNA molecules harboring a bead were extended to a slightly longer length (14 μm; $\langle X \rangle / L = 0.88$), corresponding to ~2 pN of force. This difference in relative extended length was attributed to the additional hydrodynamic force caused by the 1.5 μm dia. bead. After visually identifying a labeled DNA, the bead was captured in the optical trap. When flow was stopped, the trapped bead and its associated DNA remained visible, whereas all other DNA molecules diffused out of the evanescent field and could no longer be visualized, confirming that the bead-labeled DNA was trapped. (Fig. 2A, middle panel).

We next stretched the DNA to determine how much force the molecules could resist before rupturing (Fig. 2A, lower panel). Molecules labeled with a single biotin/digoxigenin detached from the bilayer when they were stretched to moderate lengths (Fig. 2). In all cases, the DNA remained bound to the bead, indicating that rupture occurred at or near the lipid bilayer (lower panel in Fig. 2A, B, and see below). We then measured the mean extension at which single DNA molecules were pulled free from the bilayer, which revealed that the DNA molecules were pulled free from the bilayer at a mean extended length of 16.8 ± 0.9 μm (Fig. 2C). Based on force-extension curves of dsDNA, 16.8 ± 0.9 μm corresponds to an estimated rupture force of ~20 pN, with values ranging from 5 to 40 pN as determined from the FWHM of a Gaussian fit to the data (Fig. 2C) [7,24,25]. The broad distribution of values associated with this estimated force arises from the sharp increase in the force–extension curve of λ-DNA between 15 and 18 μm [7,24,25].

We next considered which of component was most likely to rupture when force was applied. First, the DNA could potentially experience YOYO1-induced photodamage. DNA breaks arising from photodamage would be expected to occur randomly through-

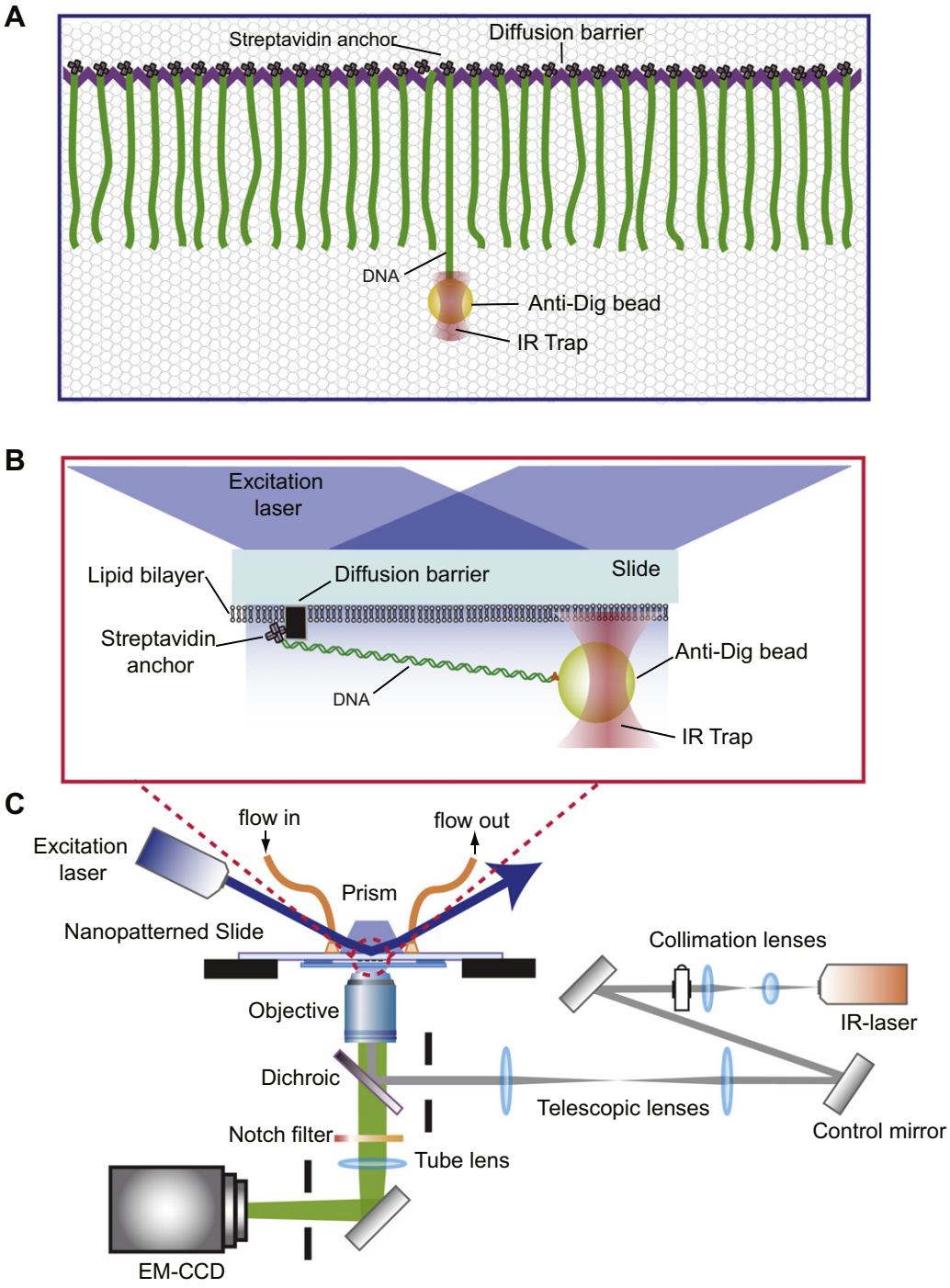

Fig. 1. Visualizing DNA curtains with a combined optical trap and TIRFM. (A) Top view and (B) side view of experimental schematic for making force measurements on DNA molecules aligned at a nanofabricated barrier on a lipid bilayer coated surface. The DNA is anchored to the bilayer through a biotin–streptavidin linkage, and its downstream end is linked to a bead that is captured in an optical trap. (C) Schematic overview of the instrument design. Full details are presented in the text.

out length of the DNA. However, this was not observed, rather the DNA most commonly ruptured near the barriers, arguing against rupture due to DNA photodamage. Second, the observation that the DNA detaches from the bilayer, but remains bound to the bead, argues that the interaction between the digoxigenin and the anti-dig coated bead are not disrupted. Third, we cannot exclude the possibility that the biotin–streptavidin interactions are disrupted. However, the biotin–streptavidin interaction can withstand at least 60 pN of force, and the binding strength between biotin and streptavidin has been reported to be as high as >200 pN [29–31], arguing against breakage of the biotin–streptavidin interaction in our experiments. Based upon these considerations, we consider the most likely conclusion to be that the DNA ruptures from the surface due to single lipids being pulled from the bilayer. This conclusion is strengthened by our finding that when the DNA is anchored to multiple lipids can no longer be pulled free from the surface (see below). Finally, the finding that extra biotin tags prevent DNA rupture under tension also rules out the possibility that

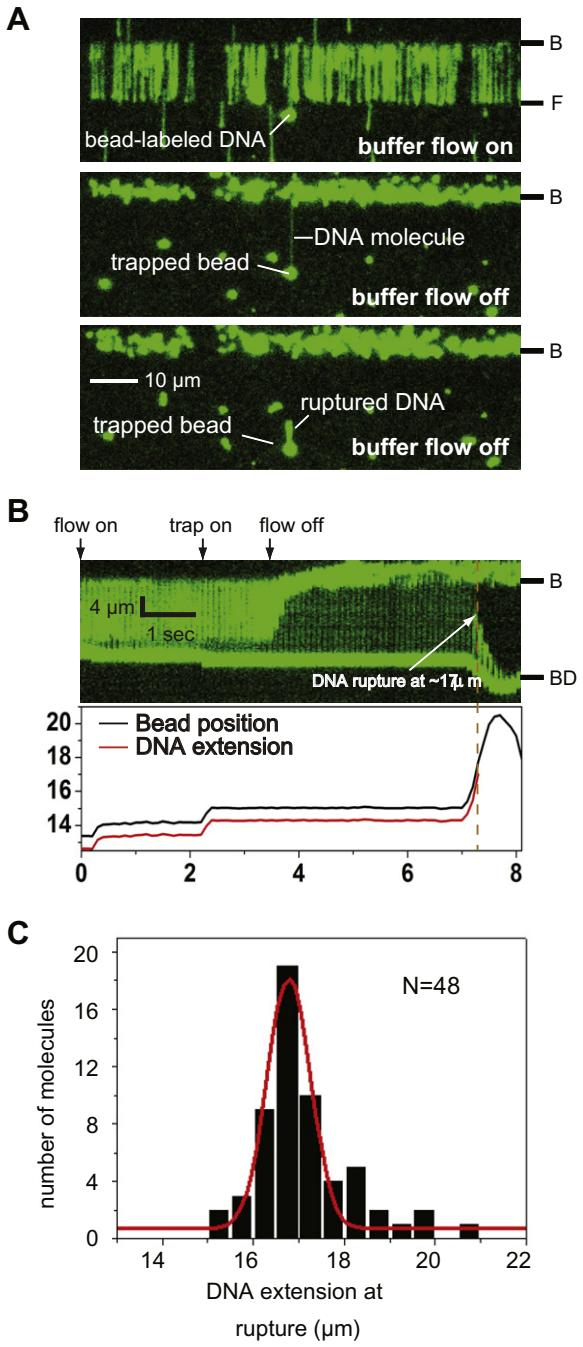

Fig. 2. Low force rupture of DNA molecules anchored to the bilayer through a single biotin–streptavidin. (A) TIRFM image of a DNA curtain aligned at a nanofabricated barrier (upper panel). In the presence of buffer flow the DNA molecules (green) can all be viewed along their full contour length, and beads are readily identified by visual inspection. When flow is terminated, the trapped bead and the corresponding DNA molecule remain extended, whereas all other DNA molecules retract from the surface (middle panel). When force is applied, the DNA is pulled free from the bilayer and remains bound to the trapped bead (lower panel). The barrier position and free end of DNA are marked as "B" and "F", respectively. (B) The upper panel shows a kymograph of a single DNA rupturing under applied tension, and the low panel shows corresponding traces of the bead (black) and DNA extension (red). In the kymograph, the fluorescence signal abruptly decreases when buffer flow because adjacent DNA molecules that are not attached to the bead disappear from view. The barrier and bead positions are marked as "B" and "BD", respectively. The orange dashed line indicates the DNA rupture from bilayer. (C) Histogram showing the distribution of lengths at which the DNA molecules are pulled free from the bilayer.

rupture events reflect YOYO1-induced photodamage. If the rupture were due to DNA photodamage, then the addition of extra biotins to the DNA end should not eliminate rupture from the surface under applied tension.

3.2. DNA molecules labeled with multiple tags resist detachment from the bilayer

The finding that lipid rupture occurs around 20 pN is problematic for experiments using the optical tweezers combined with DNA curtains because many relevant protein–DNA interactions can only be studied at higher force regimes [5,11,32–34]. We reasoned that the strength of the attachment could be enhanced by increasing the number of contacts with bilayer. We therefore made DNA molecules bearing multiple anchor points (Fig. 3). As anticipated, molecules bearing multiple attachment points were resistant to force-induced rupture and could be repeatedly stretched and relaxed without detaching from the bilayer (Fig. 3A and B). The maximum extension observed in these experiments was 26.1 ± 0.3 μm (Fig. 3C), corresponding to the transition from B-form to S-form DNA, which is a characteristic transition that takes place when DNA is overstretched beyond the normal length of B-form DNA [24,25]. The conclusion that the DNA has undergone the B–S transition is corroborated by the reversible, linear increase in YOYO1 fluorescence signal that begins when the DNA was stretched more than ~1.5-fold beyond the mean extended contour length ($\langle X \rangle / L$) for B-form DNA (Fig. 3A, compare middle and lower panels; Fig. 3B and C, inset). Previous studies have suggested this increase in signal intensity occurs because YOYO1 more readily intercalates between base pairs when the DNA is stretched to S-form [12]. The B–S transition occurs at a force of ~65 pN [24,25], thus we infer that the multi-anchor DNA molecules can withstand at least this amount of force without detaching from the bilayer. Once DNA has undergone the B–S transition, small increases in force induce significant increases in DNA length [24,25], and as a consequence we could not measure the maximum amount of force the multi-anchor DNA molecules could withstand before being pulled free from the bilayer.

3.3. Combined TIRF-trap measurements with RNA polymerase

The TIRF-trap microscope offers the ability to visualize proteins and DNA while concurrently observing their responses to applied force. As a proof-of-principle, we examined the force-induced response of quantum dot (QD) tagged RNA polymerase (RNAP) (Fig. 4A and B). QD-RNAP was injected into the sample chamber and allowed to bind to the DNA curtains, as described [17]. A bead-labeled DNA was then trapped and flow was terminated. To confirm that the QD-tagged RNAP was bound to the bead-labeled DNA, we moved the bead laterally and verified that QD-RNAP tracked with the lateral movement of the YOYO1-stained DNA (Fig. 4A). We next stretched and relaxed the DNA at a constant speed of 4.8 μm s^{-1}. Fig. 4A shows repeated extensions of a single DNA bound by several molecules of QD-tagged RNAPs in a buffer containing 25 mM KCl. At this low salt concentration QD-RNAP bound to both specific and nonspecific sites, as expected [17]. At low ionic strength both promoter-bound and nonspecifically-bound RNAP remained on the DNA through multiple stretching and relaxation cycles and the proteins remained bound even though the DNA was stretched beyond the B–S transition (Fig. 4A). We observed a total of 59 molecules of DNA-bound RNAP (41 bound to promoter sites and 18 at nonspecific sites) at low ionic strength, and none of these proteins dissociated from the DNA when it was stretched repeatedly beyond the B–S transition.

We next examined RNAP at a higher ionic strength. At 150 mM KCl, most RNAP (93%, 28/30) was bound to the promoter sites, indicating that nonspecific binding was suppressed at more physiologically relevant salt concentrations, as expected [17]. Approximately 39% of the promoter-bound RNAP (11/28) dissociated from the

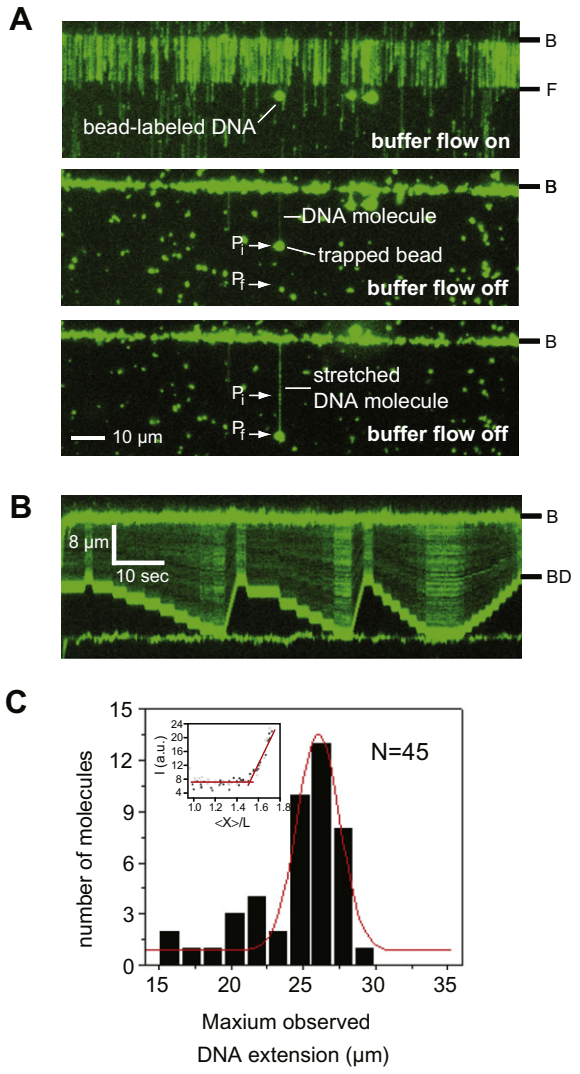

Fig. 3. Stretching DNA molecules that are attached to the bilayer by multiple anchor points. (A) TIRFM image of a DNA curtain, in which the molecules are linked to the bilayer through multiple biotin–streptavidin linkages. All molecules are extended when flow is applied (upper panel), but only the trapped molecule remains visible when flow is terminated (middle panel). As the force is applied to DNA by optical trap, the DNA is stretched beyond B–S transition without detaching from the surface (low panel). (B) Kymogram showing a DNA being repeatedly stretched and relaxed from 15 to 26 μm in length without being pulled free from the bilayer. The increase in fluorescence signal at extended lengths, corresponds to the increased binding of YOYO1 when the DNA undergoes the B–S transition. At the shortest lengths, a decrease in tension allows the time-averaged position of the DNA to penetrate more deeply into the evanescent field, which also results in an increase in fluorescence signal. (C) Histogram showing the maximum extended lengths ($N = 45$). These DNA molecules were not pulled free from the bilayer. The inset shows the median intensity of DNA fluorescence (I; in arbitrary units, $\times 10^3$) of a typical DNA molecule as a function of its relative mean extension ($\langle X \rangle / L$). Closed squares (■) represent the intensity as the molecule was being stretched, and open circles (○) represent the intensity as the same molecule was being relaxed.

DNA during the stretching and relaxation cycles when the ionic strength was increased to 150 mM KCl (Fig. 4B), yielding a lifetime for the promoter-bound proteins of <1 min when the DNA was stretched beyond the B–S transition. Interestingly, in the same flow cells, RNAP bound to DNA lacking a bead and stretched only by flow force (~0.5 pN) remained bound to the DNA for >7 min, as expected based on previous results [17]. These results show that DNA-bound RNAP complexes are more readily destabilized when the DNA template is stretched beyond the B–S transition under physiological salt conditions.

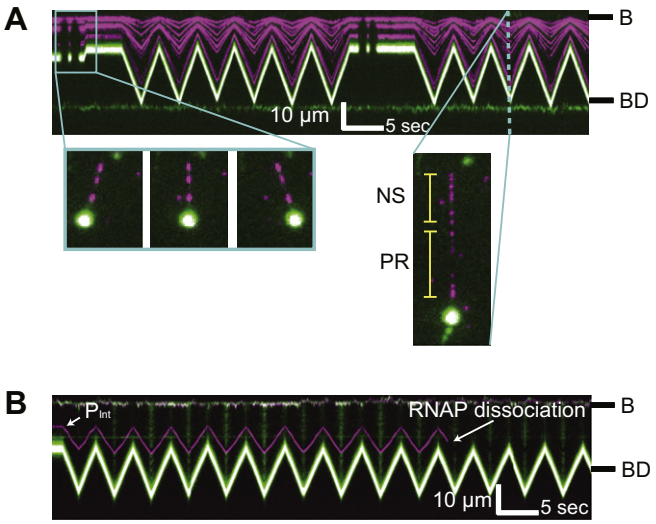

Fig. 4. Response of RNAP to DNA stretching. (A) Representative kymograph showing stretching and relaxation of DNA bound by QD-tagged RNAP (magneta) in buffer containing 25 mM KCl. The DNA was repeatedly stretched and relaxed at a constant speed 4.8 μm s^{-1}. The bead (green) was laterally moved to confirm that the proteins were bound to DNA (highlighted). Promoter and nonspecific sites are highlighted as "PR" and "NS", respectively. (B) Kymograph showing repeated stretching at 150 mM KCl. One RNAP (magenta) was bound to a promoter and dissociated after several cycles of stretching and relaxation of DNA as evident by loss of QD. The barrier position and bead are marked as "B" and "BD", respectively.

The work described here involved development of a combined TIRF-trap microscope for probing the physical properties of individual DNA molecules aligned into DNA curtains at nanofabricated barriers to lipid diffusion. This instrument allowed us to estimate the force required to pull a single molecule of biotin-DPPE from a supported lipid bilayer and also establishes methodologies necessary for making force based measurements on the lipid-tethered DNA molecules within the DNA curtains. The forces that maintain lipids within lipid bilayers have been previously investigated both at the experimental and theoretical levels [35,36]. Evans et al. reported that the lipid rupture force is 20 ± 7 pN for receptor dissociation from the cell membrane using biomembrane force spectroscopy [36], which is in excellent agreement with our results, supporting the conclusion that force-induced DNA detachment from the DNA curtains reflects the extraction of single lipid from the bilayer. The addition of multiple attachment point to the bilayer allowed single molecules to be stretched with ⩾65 pN without being pulled free from the bilayer. However, the primary advantage of DNA curtains as an experimental platform lies in the ability to directly visualize hundreds of individual DNA molecules, and to take full advantage of the statistical power of DNA curtains will require future development of a system in which multiple optical (or magnetic) traps that can be used to simultaneously capture all of the DNA molecules within a field-of-view.

Acknowledgments

This research was funded in part by the Initiatives in Science and Engineering (ISE; awarded to E.C.G. and S.W.) program through Columbia University, and by NIH grants (GM074739 and GM 082848) to E.C.G. In addition, E.C.G. is an Early Career Scientist with the Howard Hughes Medical Institute. This work was partially supported by the Nanoscale Science and Engineering Initiative of the National Science Foundation under NSF Award No. CHE-0641523 and by the New York State Office of Science, Technology, and Academic Research (NYSTAR). J.Y.L. was supported in part by the Korea Research Foundation Grant funded by the Korean

Government (KRF-2008-357-C00048). T.A.F. was supported by an NSF Graduate Research fellowship.

Appendix A. Supplementary data

Supplementary data associated with this article can be found, in the online version, at http://dx.doi.org/10.1016/j.bbrc.2012.08.127.

References

[1] I. Tinoco, R.L. Gonzalez, Biological mechanisms, one molecule at a time, Genes & Development 25 (2011) 1205–1231.
[2] X.S. Xie, P.J. Choi, G.W. Li, N.K. Lee, G. Lia, Single-molecule approach to molecular biology in living bacterial cells, Annual Review of Biophysics 37 (2008) 417–444.
[3] A.M. van Oijen, Single-molecule approaches to characterizing kinetics of biomolecular interactions, Current Opinion in Biotechnology 22 (2011) 75–80.
[4] C. Joo, H. Balci, Y. Ishitsuka, C. Buranachai, T. Ha, Advances in single-molecule fluorescence methods for molecular biology, Annual Review of Biochemistry 77 (2008) 51–76.
[5] M.D. Brenner, R.B. Zhou, T. Ha, Forcing a connection: impacts of single-molecule force spectroscopy on in vivo tension sensing, Biopolymers 95 (2011) 332–344.
[6] K.C. Neuman, A. Nagy, Single-molecule force spectroscopy: optical tweezers, magnetic tweezers and atomic force microscopy, Nature Methods 5 (2008) 491–505.
[7] T.R. Strick, J.F. Allemand, D. Bensimon, V. Croquette, Stress-induced structural transitions in DNA and proteins, Annual Review of Biophysics and Biomolecular Structure 29 (2000) 523–543.
[8] A. Candelli, W.G.J. L., E.J.G. Peterman, Combining optical trapping, fluorescence microscopy and microfluidics for single molecule studies of DNA–protein interactions, Physical Chemistry Chemical Physics 13 (2011) 7263–7272.
[9] R.B. Zhou, M. Schlierf, T. Ha, Force fluorescence spectroscopy at the single-molecule level, methods in enzymology, Vol 475: Single Molecule Tools Pt B 474 (2010) 405–426.
[10] C.U. Murade, V. Subramaniam, C. Otto, M.L. Bennink, Force spectroscopy and fluorescence microscopy of dsDNA-YOYO-1 complexes: implications for the structure of dsDNA in the overstretching region, Nucleic Acids Research 38 (2010) 3423–3431.
[11] J. Van Mameren, M. Modesti, R. Kanaar, C. Wyman, G.J.L. Wuite, E.J.G. Peterman, Dissecting elastic heterogeneity along DNA molecules coated partly with Rad51 using concurrent fluorescence microscopy and optical tweezers, Biophysical Journal 91 (2006) L78–L80.
[12] C.U. Murade, V. Subramaniam, C. Otto, M.L. Bennink, Interaction of oxazole yellow dyes with DNA studied with hybrid optical tweezers and fluorescence microscopy, Biophysical Journal 97 (2009) 835–843.
[13] E.C. Greene, S. Wind, T. Fazio, J. Gorman, M.L. Visnapuu, DNA curtains for high-throughput single-molecule optical imaging, methods in enzymology, Vol 472: Single Molecule Tools Pt A: Fluorescence Based Approaches 472 (2010) 293–315.
[14] M.L. Visnapuu, T. Fazio, S. Wind, E.C. Greene, Parallel arrays of geometric nanowells for assembling curtains of DNA with controlled lateral dispersion, Langmuir 24 (2008) 11293–11299.
[15] T. Fazio, M.L. Visnapuu, S. Wind, E.C. Greene, DNA curtains and nanoscale curtain rods: high-throughput tools for single molecule imaging, Langmuir 24 (2008) 10524–10531.
[16] J.Y. Lee, E.C. Greene, Assembly of recombinant nucleosomes on nanofabricated DNA curtains for single-molecule imaging, Methods in Molecular Biology 778 (2011) 243–258.
[17] I.J. Finkelstein, M.L. Visnapuu, E.C. Greene, Single-molecule imaging reveals mechanisms of protein disruption by a DNA translocase, Nature 468 (2010) 983–987.
[18] J. Gorman, A.J. Plys, M.L. Visnapuu, E. Alani, E.C. Greene, Visualizing one-dimensional diffusion of eukaryotic DNA repair factors along a chromatin lattice, Nature Structural & Molecular Biology 17 (2010) 932–U937.
[19] M.L. Visnapuu, E.C. Greene, Single-molecule imaging of DNA curtains reveals intrinsic energy landscapes for nucleosome deposition, Nature Structural & Molecular Biology 16 (2009) 1056–U1075.
[20] F.M. Fazal, S.M. Block, Optical tweezers study life under tension, Nature Photonics 5 (2011) 318–321.
[21] L. Bai, T.J. Santangelo, M.D. Wang, Single-molecule analysis of RNA polymerase transcription, Annual Review of Biophysics and Biomolecular Structure 35 (2006) 343–360.
[22] J.W. Shaevitz, E.A. Abbondanzieri, R. Landick, S.M. Block, Backtracking by single RNA polymerase molecules observed at near-base-pair resolution, Nature 426 (2003) 684–687.
[23] M.D. Wang, M.J. Schnitzer, H. Yin, R. Landick, J. Gelles, S.M. Block, Force and velocity measured for single molecules of RNA polymerase, Science 282 (1998) 902–907.
[24] S.B. Smith, Y.J. Cui, C. Bustamante, Overstretching B-DNA: the elastic response of individual double-stranded and single-stranded DNA molecules, Science 271 (1996) 795–799.
[25] S.B. Smith, L. Finzi, C. Bustamante, Direct mechanical measurements of the elasticity of single DNA-molecules by using magnetic beads, Science 258 (1992) 1122–1126.
[26] J.R. Wenner, M.C. Williams, I. Rouzina, V.A. Bloomfield, Salt dependence of the elasticity and overstretching transition of single DNA molecules, Biophysical Journal 82 (2002) 3160–3169.
[27] C.G. Baumann, S.B. Smith, V.A. Bloomfield, C. Bustamante, Ionic effects on the elasticity of single DNA molecules, Proceedings of the National Academy of Sciences of the United States of America 94 (1997) 6185–6190.
[28] I.D. Vladescu, M.J. McCauley, M.E. Nunez, I. Rouzina, M.C. Williams, Quantifying force-dependent and zero-force DNA intercalation by single-molecule stretching, Nature Methods 4 (2007) 517–522.
[29] H. Grubmuller, B. Heymann, P. Tavan, Ligand binding: molecular mechanics calculation of the streptavidin biotin rupture force, Science 271 (1996) 997–999.
[30] M.J. Lang, P.M. Fordyce, A.M. Engh, K.C. Neuman, S.M. Block, Simultaneous, coincident optical trapping and single-molecule fluorescence, Nature Methods 1 (2004) 133–139.
[31] E.A. Shank, C. Cecconi, J.W. Dill, S. Marqusee, C. Bustamante, The folding cooperativity of a protein is controlled by its chain topology, Nature 465 (2010) 637–U134.
[32] D.E. Smith, Single-molecule studies of viral DNA packing, Current Opinion in Virology 1 (2011) 134–141.
[33] C. Bustamante, Y.R. Chemla, N.R. Forde, D. Izhaky, Mechanical processes in biochemistry, Annual Review of Biochemstry 73 (2004) 705–748.
[34] J. Bednar, S. Dimitrov, Chromatin under mechanical stress: from single 30 nm fibers to single nucleosomes, FEBS Journal 278 (2011) 2231–2243.
[35] S.-J. Marrink, O.T. Berger, P. Tieleman, F. Jähnig, Adhesion forces of lipids in a phospholipid membrane studied by molecular dynamics simulations, Biophysical Journal 74 (1998) 931–943.
[36] E. Evans, D. Berk, A. Leung, N. Mohandas, Detachment of agglutinin-bonded red blood cells. II. Mechanical energies to separate large contact areas, Biophysical Journal 59 (1991) 849–860.